# Pre-and postoperative cerebral blood flow changes in patients with idiopathic normal pressure hydrocephalus measured by computed tomography (CT)-perfusion

**Doerthe Ziegelitz[1], Jonathan Arvidsson[2,3], Per Hellström[4], Mats Tullberg[4], Carsten Wikkelsø[4] and Göran Starck[2,3]**

## Abstract

In idiopathic normal pressure hydrocephalus (iNPH), the cerebral blood flow (CBF) is of pathophysiological interest and a potential biomarker. Computed tomography perfusion (CTP), an established technique with high spatial resolution and quantitative measurements, has not yet been used in the iNPH context. If CTP were sensitive to the CBF levels and changes in iNPH, this technique might provide diagnostic and prognostic absolute perfusion thresholds. The aim of this work was to determine the applicability of CTP to iNPH. CBF measurements of 18 patients pre- and 17 three months postoperatively, and six healthy individuals (HI) were evaluated in 12 cortical and subcortical regions of interest. Correlations between CBF and symptomatology were analyzed in shunt-responders. Compared to HI, the preoperative CBF in iNPH was significantly reduced in normal appearing and periventricular white matter (PVWM), the lentiform nucleus and the global parenchyma. No CBF differences were shown between responders and non-responders. In responders, the CBF recovered postoperatively by 2.5–32% to approximately the level of HI, but remained significantly decreased in the PVWM of non-responders. The pre- and postoperative CBF of cortical and subcortical regions correlated with the intensity of symptoms. In spite of limited spatial coverage, CTP can measure CBF changes in iNPH.

## Introduction

Idiopathic normal pressure hydrocephalus (iNPH) is a disorder characterized by gait- and balance problems, cognitive impairment, and urge/incontinence in conjunction with a communicating hydrocephalus on imaging and a normal intracranial pressure.[1] It is one of few treatable causes of dementia and more than 80% of the patients improve after shunt surgery. The disease is under-diagnosed and under-treated.

The cerebral blood flow (CBF) has a central role in the pathophysiology of iNPH as indicated by preoperative CBF reduction in the cerebral cortex, central grey matter (GM) structures and the periventricular white matter (PVWM),[2–6] postoperative CBF restoration in patients with favorable clinical outcome,[7–11] and correlation of the CBF alterations with symptoms and signs of iNPH.[6,8,11,12]

[1]Department of Neuroradiology, Institute of Clinical Sciences, Sahlgrenska University Hospital, Gothenburg, Sweden
[2]Department of Radiation Physics, Institute of Clinical Sciences, Sahlgrenska University Hospital, Gothenburg, Sweden
[3]Medical Physics and Biomedical Engineering, Sahlgrenska University Hospital, Gothenburg, Sweden
[4]Department of Clinical Neuroscience and Rehabilitation, Institute of Neuroscience and Physiology, The Sahlgrenska Academy at the University of Gothenburg, Sweden

**Corresponding author:**
Doerthe Ziegelitz, Department of Neuroradiology, Sahlgrenska University Hospital, SE-41345 Gothenburg, Sweden.
Email: doerthe.ziegelitz@vgregion.se

In the context of iNPH, mainly xenon computed tomography (xenon CT), single photon emission computed tomography (SPECT) and positron emission tomography (PET) have been used. These techniques suffer from disadvantages such as unwanted side effects (xenon CT), insensitivity to deep structures (SPECT), suboptimal spatial resolution (SPECT, PET) and low accessibility (xenon CT, PET). Newer perfusion methods like magnetic resonance perfusion (MRP) and computed tomography perfusion (CTP) that do not have these disadvantages might be better suited to identify a perfusion-based imaging marker.

MRP studies based on T2* bolus tracking have reproduced earlier CBF findings in iNPH patients,[6,11,13] but also highlighted the problem of relative perfusion values[6] and of postoperative susceptibility artifacts due to metallic shunt valve components.[11] A single MRP study used the arterial spin labeling technique for CBF estimation in iNPH patients.[14] Although this is a promising technique, it requires imaging at 3 Tesla, which could potentially further accentuate the susceptibility artifacts.

CTP is generally considered to report perfusion values in absolute terms,[15–17] is more available than MRP, and metal streak artifacts from the shunt should be negligible. However, so far CTP has not been applied to iNPH. If CTP demonstrated sensitivity to the CBF levels and expected CBF changes in iNPH, this technique might provide absolute diagnostic and prognostic perfusion thresholds and could be easily implemented into clinical praxis as CT usually is the first radiologic examination in cases of suspected iNPH.

The aim of the present work was to examine the pre- and postoperative regional and global perfusion in iNPH by CTP in relationship to the symptomatology of the disease. The hypothesis was that CTP is capable of detecting the expected perfusion changes in iNPH.

## Materials and Methods

### Patients and healthy individuals

Between September 2005 and December 2008, 51 patients with suspected iNPH, referred to our hydrocephalus unit for preoperative examination, were prospectively recruited to this study. Written informed consent was obtained from the patients or their next of kin. All patients underwent CTP and MRP on two consecutive days, prior to and three months after shunt insertion. Only subjects whose pre- and postoperative MRP and CTP were technically successful remained in the study. The MRP results have been published earlier.[6,11]

The patients had neuropsychological, physiotherapeutic, and neurological examinations. Performance was assessed in the four domains of gait, neuropsychology, balance and continence yielding separate scores as well as a total score on a recently published iNPH scale.[18] The diagnosis of probable iNPH was based on the iNPH Guidelines[1] requiring a gait disturbance in combination with cognitive and/or urinary symptoms, communicating hydrocephalus on imaging, and absence of a known cause of hydrocephalus. The imaging criteria were assessed on MRI and comprised an Evans' index $>0.3$ that was not entirely caused by atrophy, the absence of macroscopic obstruction of the cerebrospinal fluid circulation, visible aqueductal and fourth ventricular flow void, a corpus callosum angle of $> 40°$ and $< 90°$ and narrow sulci at the vertex.

Thirty-two patients were diagnosed with probable iNPH, but three of these withdrew their consent and one died prior to shunt insertion. Ten patients had to be excluded due to technical or procedural problems: incomplete or unsuccessful MRI ($n = 6$), motion artifacts on MRP ($n = 2$), wrongly centred preoperative CTP and motion artifacts on postoperative CTP ($n = 1$), preoperative CTP motion artifacts and postoperative CTP not performed ($n = 1$). One patient developed a minor, postoperative right-sided subdural hematoma, which was treated conservatively. This patient's post-operative CTP was omitted from the study. Thus, 18 pre- and 17 postoperative CTP provided the iNPH data reported here.

All patients received a programmable ventriculo-peritoneal shunt, either a Codman Hakim™ Valve (Codman Johnson & Johnson, New Jersey 08933, USA) or a Strata™ Valve (Medtronic PS Medical, Santa Barbara, USA), placed in either the right frontal lobe ($n = 19$) or the right parieto-occipital region ($n = 1$).

The patients were re-evaluated three months after surgery in the same way as preoperatively. Improvement was defined as an increase of at least five iNPH scale score points which represents a substantial clinical improvement.[18] Patients who fulfilled this criterion constituted the shunt-responder group, and the remaining patients were considered non-responders.

Six age-matched healthy individuals (HI) were consecutively included into the study as controls out of a cohort of 16, and provided the normal level of regional and global CBF. The recruitment process of these HI has been published in an earlier study.[6]

Demographic data, Evans' index and Wahlund's rating score[19] for white matter (WM) changes of the HI and iNPH patients, as well as clinical data for the latter group, are shown in Table 1.

The Regional Ethics Committee of Gothenburg and the Radiation Protection Committee of the Sahlgrenska University Hospital approved the study. The Swedish

**Table 1.** Demographic data, Evans' index, and Wahlund's rating score for white matter (WM score) changes for the healthy individuals and the iNPH patients, as well as clinical data for the iNPH group.

| | Healthy individuals (n = 6) | Responders (n = 13) | Non-responders (n = 5) |
|---|---|---|---|
| Age in years, mean (range) | 71 (68–74) | 71 (59–82) | 69 (55–80) |
| Sex, men/women | 4/2 | 6/7 | 4/1 |
| Hypertension, yes/no | 0/6 | 3/10 | 2/3 |
| Symptom duration in months, mean (range) | | 39 (7–168) | 22 (18–24) |
| Preoperative iNPH scale score, mean (range) | | 46 (8–92) | 65 (38–94) |
| Postoperative iNPH scale score, mean (range) | | 67 (39–99) | 62 (37–93) |
| Preoperative EI, mean (±SD) | 0.28 (±0.02) | 0.41 (±0.06) | 0.42 (±0.04) |
| Postoperative EI, mean (±SD) | | 0.38 (±0.06) | 0.41 (±0.03) |
| Preoperative WM score, mean(±SD) | 6.8 (±1.7) | 6 (±4.9) | 7.2 (±5.8) |
| Postoperative WM score, mean (±SD) | | 5.9 (±5) | 6.6 (±6.3) |

SD = standard deviation.

research ethics review system is regulated by law, i.e. the Act on Ethical Review of Research Involving Humans.

## Imaging

At baseline, CBF was measured in all subjects using CTP and MRP on two consecutive days at the same time of day to reduce diurnal fluctuations. The intake of nicotine and caffeine prior to imaging were not restricted per protocol. On the same terms, CTP and MRP were repeated in the patient group three months after shunt insertion.

For CTP, we used a CT unit with a 16-channel multi detector array (Lightspeed PRO 16; General Electric, Milwaukee, WI, USA). The bolus consisted of an injection of 50 mL iopromide (300 mg iodine/ mL, Ultravist, Schering, Berlin, Germany) at a rate of 4 mL/ s, followed by a saline flush, into the same antecubital vein as during perfusion day one. Scanning was initiated 5 s after the start of the bolus injection. The examination covered four adjacent 5-mm sections immediately above the posterior commissure, parallel to a line between the posterior commissure and the root of the nose. The acquisition parameters were 80 kV, 200 mA, 99 scans, four images per cine scan, scan repetition time 0.5 s, acquisition time 50 s, FOV 250 mm, and matrix $512 \times 512$.

The MR protocol included besides the MRP a transverse fluid-attenuated inversion-recovery (FLAIR) sequence (TE 100 ms, TR 9000 ms, IR delay 2500 ms, slice thickness 3 mm, no gap, 44 slices, FOV 230 mm, image acquisition matrix $192 \times 192$ reconstructed to $256 \times 256$).

In the context of the evaluation of the MRP data published earlier,[6,11] regions of interest (ROIs) had been delineated on these FLAIR images (see section below for further details of the ROIs used in this study). Those same ROIs were applied to evaluate the CTP data.

## Post-processing

*Perfusion calculation.* Perfusion calculations were performed off-line with in-house developed software running on MATLAB (Math Works, Natick, MD, USA), utilizing a batch processing framework (pipeline) (Danish Research Centre for Magnetic Resonance, Copenhagen University Hospital Hvidovre, Danmark).

The AIF was obtained in the left hemisphere from the M2 segment of the middle cerebral artery. Among the voxels with the highest contrast concentration, one voxel with the largest peak height and the least width was chosen manually by an experienced neuroradiologist.

The VOF consisted of four voxels, manually placed centrally in the superior sagittal sinus or the confluence of sinuses to ensure absence of partial volume effects.

The attenuation-to-time curves were obtained as the average CT-number in each ROI. The first pass of contrast agent was extracted by fitting a gamma variate function to the bolus passage peak in the attenuation-to-time curve. Similarly, the arterial input function (AIF) and venous output function (VOF) were obtained as the attenuation-to-time gamma variate curves in the voxels selected for this purpose. The AIF was then scaled so that the area under the curve (AUC) was equal to the AUC of the VOF. Deconvolution of the parenchyma attenuation-to-time curve with the AIF by block-circulant singular value decomposition (cSVD)[20] and a global noise threshold

of 0.05 yielded the tissue residue function scaled with CBF. This function was normalized to the density of brain tissue and corrected for the difference in haematocrit between large and small vessels by multiplying by a factor of 0.71.[21] CBF and CBV were determined as the maximum and the area under this curve, respectively.[22]. Mean transit time (MTT) was obtained as the ratio of CBV/CBF according to the central volume theorem.[23]

*Co-registering and re-sampling.* A mean CT image was calculated from 10 s of the scan centered on the concentration peak in the parenchyma. Rigid co-registering of the FLAIR images with this mean CT image was performed manually by an experienced neuroradiologist using the 3DSlicer software (ver. 4.3, http://www.slicer.org).[24] The FLAIR images and all ROIs were subsequently re-sampled to the mean CT image using the open source software package NiftyReg.[25,26] The ROIs were then applied to the attenuation-to-time series data together with a vessel mask. The vessel mask was calculated on a peak concentration image obtained from the attenuation-to-time series. Noise in the peak concentration image was reduced by means of bi-lateral filtering. All voxels with a value greater than 2.2 times the position of the single peak in the histogram were included in the vessel mask.

Furthermore, the ROIs re-sampled to the perfusion scan were trimmed such that border voxels that were filled to less than 90% with the original FLAIR ROI were discarded.

*Regions of interest.* The ROIs applied to this CTP data were identical with ROIs that had been drawn for previous MRP studies on the same subjects[6,11] (Figure 1).

In those previous MRP studies,[6,11] 11 different ROIs had been manually delineated by one neuroradiologist on all sections of the FLAIR sequence that contained the respective anatomical structure.

The 11 ROIs covered: occipital cortex, anterior cingulate gyrus, caudate head, lentiform nucleus, periventricular thalamus, central thalamus, normal appearing white matter (NAWM), anterior and posterior periventricular white matter (PVWM), hippocampus, and basal medial frontal cortex.

A 12th ROI that delineated the global parenchyma was automatically computed. On the voxel histogram of the noise filtered mean CT image, a threshold between the CSF and parenchyma peaks was defined and applied in combination with the vessel mask.

The ROIs were combined according to their tissue characterization to a central grey matter ROI (central GM = caudate head, lentiform nucleus, periventricular and central thalamus) and a total periventricular white matter ROI (Total PVWM = PVWMant and PVWMpost).
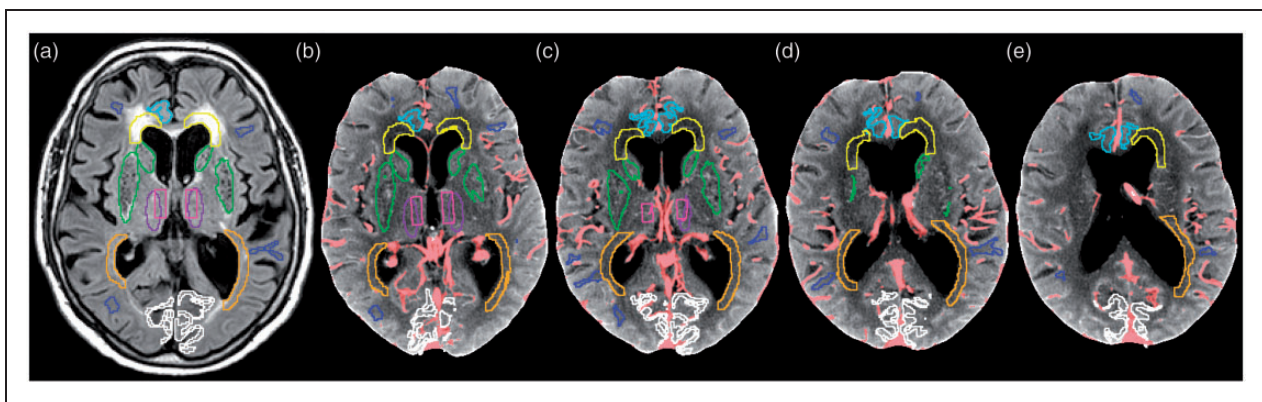


**Figure 1.** (a–e) Postoperative FLAIR and mean CT image of an iNPH patient illustrating the position of the manually drawn regions of interest (ROIs). Image (a) shows one trans-axial section of the FLAIR sequence, at the level of the basal ganglia, illustrating the position of the manually drawn ROIs. Images (b–e) are mean CT images, representing the sampled four consecutive 5-mm CTP sections at the level of the basal ganglia and the cella media. After the co-registering and the re-sampling of the FLAIR images with the ROIs to the mean CT image, some ROIs are delineated partly in different sections due to tilting of the head. No metallic streak artifacts are present. The light pink pixels in (b–e) are discarded by the vessel mask.
ROI-key: blue = normal appearing white matter (NAWM); turquoise = cingulate gyrus; yellow = anterior periventricular white matter (PVWMant); orange = posterior periventricular white matter (PVWMpost); light green = caudate head; dark green = lentiform nucleus; dark rose = central thalamus; pink = periventricular thalamus; white = occipital cortex The global parenchyma was automatically calculated based on the voxel histogram of the mean CT image excluding CSF voxels and applied in combination with the vessel mask.

The shunt devices did not visibly degrade the image quality of the right hemisphere. Therefore, the bilateral ROIs of each anatomical region were combined and regarded as an entity in the evaluation.

The limited spatial coverage of the CTP implied that the ROIs were applicable only to parts of each anatomical structure. The hippocampus and the basal medial frontal cortex were depicted by the CTP only in singular subjects, why these ROIs were omitted from the statistical analyses.

In spite of a detailed study protocol, the placement of the 2 cm CTP slab varied to some extent and was influenced by rotation of the head. Consequently, the anatomical coverage of the imaged brain volume showed some inter- and intra-individual variance, which also led to variations of the size of the covered ROIs.

## Morphological evaluation

EI and the extent of infra- and supratentorial WM changes were determined for each individual on the transaxial FLAIR images, pre- and postoperatively. The WM changes were graded using the visual rating scale by Wahlund et al.[19] (Table 1).

## Statistical analysis

For statistical analysis, we used IBM SPSS Statistics, release version 22.

Absolute cerebral perfusion estimates were used for all statistical analyses.

Due to the small sample size and lack of normal distribution of data, only non-parametric tests were performed. Comparison of two groups was performed by Mann–Whitney U test and of three groups by the Kruskal–Wallis test. For the analysis of the postoperative changes and the comparison of the bilateral ROIs, Wilcoxon signed rank test for related samples was chosen.

Correlations between perfusion estimates and clinical performance were explored with the Spearman's rank correlation test.

Significance is stated at $p < 0.05$.

Because of the explorative nature of this study, $p$ values were not adjusted for multiple comparisons, partly because of variations in sample sizes and partly to avoid type II errors when the results displayed consistent patterns.

## Results

Fifteen patients (75%) improved between 5 and 40 score points on the iNPH scale after shunt surgery (mean 20; responders) and five patients (25%) were unchanged or deteriorated (mean −3; non-responders).

A comparative analysis of right sided versus left sided ROIs revealed no significant CBF differences (data not shown), indicating the absence of essential perfusion asymmetry between the hemispheres.

The image quality of the analyzed CTP was good, and no metal streak artifacts from the inserted shunts or any other artifacts were detected.

In HI, the median (± IQR) CBF was 13.7 (±1.1) mL/100 g/min in central GM and 6.8 (±0.6) mL/100 g/min in NAWM with a resultant GM-WM ratio of 2.0. The corresponding values for the iNPH patients are listed in Table 2. Figure 2 offers a comparative analysis of the median (±IQR) CBF values of the iNPH subgroups.

Prior to surgery, comparisons of the iNPH subgroups (Figure 2) demonstrated no significant CBF differences between iNPH shunt-responders and non-responders. Compared to HI, CBF was significantly reduced in the iNPH subgroups in the PVWMant (non-responders $p = 0.04$), the PVWMpost (non-responders $p = 0.004$; responders $p = 0.02$), as well as in the total PVWM (non-responders $p = 0.007$; responders $p = 0.03$).

When all iNPH patients were analyzed preoperatively as one group and compared to the HI, not only the PVWM demonstrated a significant CBF reduction, also the lentiform nucleus ($p = 0.048$), the NAWM ($p = 0.02$), and the parenchyma ($p = 0.01$) showed significantly decreased CBF.

On individual level, the CBF in responders increased postoperatively in all anatomical regions by 2.5–32%; significantly in the caudate head ($p = 0.047$), the NAWM ($p = 0.01$), the PVWMant ($p = 0.04$), the total PVWM ($p = 0.01$), and in the parenchyma ($p = 0.01$) (Figure 3). Due to the small sample size of the non-responder group, Wilcoxon signed rank test for related samples was not applied to this subgroup.

The responders' postoperative CBF did not differ from the HI's level of perfusion, whereas the CBF of non-responders remained significantly reduced in the PVWM (PVWMant $p = 0.02$; PVWMpost $p = 0.002$; total PVWM $p = 0.008$) (Figure 4).

**Table 2.** CTP-based median CBF values (±IQR) and the resultant GM-WM ratio for the healthy individuals (HI) and the iNPH patients.

| CBF (mL/100 g/min) | HI | iNPH |
|---|---|---|
| Central GM | 13.7 (1.1) | 11.3 (1.6) |
| NAWM | 6.8 (0.6) | 5.6 (0.7) |
| GM-WM CBF ratio | 2.0 | 2.0 |

IQR = inter quartile range, GM = grey matter, WM = white matter, NAWM = normal appearing white matter.
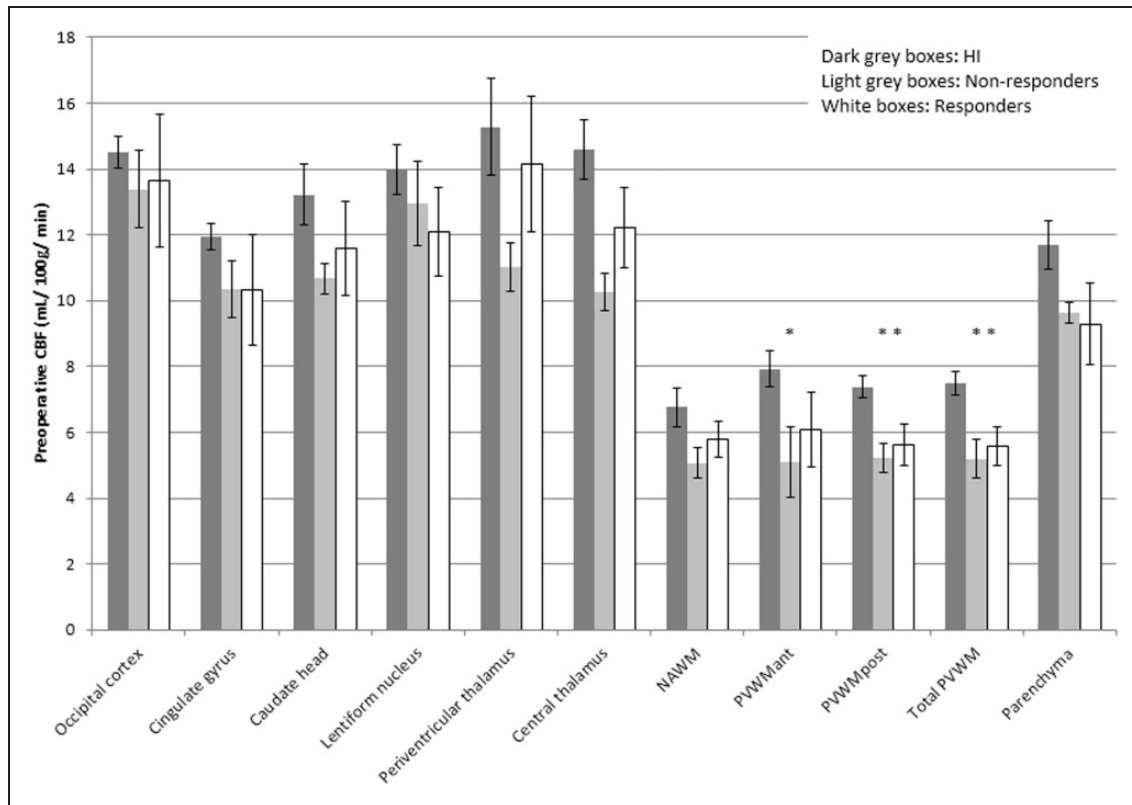
**Figure 2.** Preoperative CBF values (median, IQR) for the healthy individuals, the non-responders and the responders. Asterisks indicate significant CBF reduction as compared to HI ($p < 0.05$).
NAWM = normal appearing white matter; PVWM = periventricular white matter; ant = anterior; post = posterior.

In responders, the preoperative CBF of the periventricular WM regions, the cingulate gyrus, the occipital cortex and the parenchyma correlated with the iNPH scale score and with several domain scores. These correlations are summarized in Table 3.

In the iNPH group as a whole, preoperative regional or global CBF did not correlate with symptoms and signs of the disease.

Postoperatively, responders demonstrated a significant positive correlation between the CBF of the cingulate gyrus and the continence score and total iNPH scale score. Perfusion in the periventricular WM regions showed positive correlations with the gait score, continence score and total iNPH scale score. Further, continence was positively related to perfusion in the occipital cortex. The results are listed in Table 3.

No correlations were found between the individual postoperative CBF changes and the improvement in clinical performance (iNPH scale score and domain scores), measured as the differences between pre- and postoperative results.

Preoperatively, HI and iNPH patients showed no significant differences regarding the extent of WM lesions and no significant correlations were found between CBF and EI or WM lesion burden. The EI

and the degree of WM lesions demonstrated no significant differences between the responder and the non-responder group either pre- or postoperatively. The postoperative reduction of the EI (Table 1) was statistically significant in the responder group ($p = 0.003$), but not in the non-responder group. Neither were the postoperative reductions in WM lesions of statistical significance in responders or non-responders. No correlations were found between the postoperative CBF changes in WM and the postoperative changes in EI or WM lesion burden.

## Discussion

This is the first study testing the feasibility of CTP in iNPH. It displayed preoperative regional and global CBF reductions that, after shunt insertion, in responders were restored to approximately the perfusion levels of HI. Also, both the pre- and the postoperative CBF in the responder group correlated with the severity of symptoms.

The preoperative findings of a significant global CBF reduction and significantly decreased regional CBF in the lentiform nucleus, the PVWM and the NAWM in iNPH were in concordance with earlier
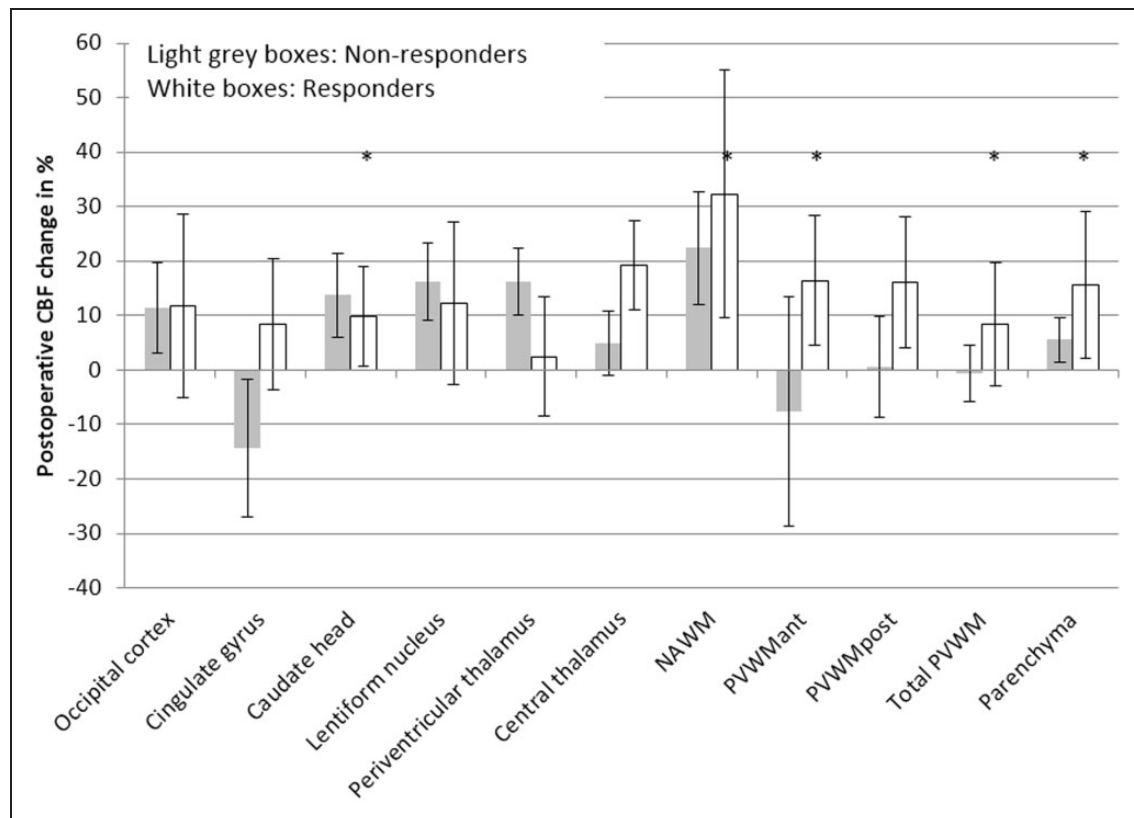
**Figure 3.** Postoperative individual CBF changes in % (median, IQR) for the responders and non-responders. Statistically significant CBF increases in the responder group are indicated by asterisks (*p* < .05).
NAWM = normal appearing white matter; PVWM = periventricular white matter; ant = anterior; post = posterior.

MRP-, SPECT- and PET-based reports.[2–6,13] The postoperative results mirrored earlier findings of a significant postoperative global[7,10,11] and regional CBF increase in central GM, deep WM[8] and in PVWM[11] in iNPH responders.

The main difference between the iNPH subgroups in this study seemed to be that responders showed recovery of the regional CBF in all anatomical regions after shunting while the non-responders' perfusion of the PVWM remained reduced and their CBF apparently decreased in the cingulate gyrus (Figures 2–4). The CBF increase in the caudate head, lentiform nucleus and the periventricular thalamus, which also the non-responders experienced after shunt insertion, equalled or exceeded in percentage and in absolute terms the increase of the responders. However, this increase effected no clinical improvement. This might either indicate that the improvement of the GM perfusion is insufficient in non-responders or that improved GM CBF is irrelevant as long as the WM regions do not recover because of permanent damage.[13,27,28] As the only significant difference between iNPH subgroups after shunting and HI was a reduced CBF in non-responders' PVWM (Figure 4), we suppose that

normal or near normal performance of the periventricular white matter tracts is a prerequisite for the functioning of the frontal periventricular cortico-basal ganglia- thalamico- cortical pathways in iNPH.[2,6,11,28,29]

In line with earlier studies on iNPH and secondary NPH,[2,3,10,28,29] the preoperative absolute thalamic and occipital perfusion of iNPH patients was reduced in relation to HI (Figure 2), even if not significantly.

In a prior postoperative MRP study on the same material,[11] the median relative CBF increase in responders was 2–9% while the CTP-based corresponding numbers were 2.5–32%. These different restoration ratios likely are the consequence of normalization of the MRP data against an internal reference. Kimura et al.[28] found a postoperative CBF restoration ranging from 19% (occipital cortex) up to 55% (frontal subcortex) in secondary NPH using xenon- CT and absolute CBF estimates. The different magnitude of CBF changes comparing the xenon-CT with CTP might be explained by disparity between the perfusion techniques and between the patient groups that were examined. Kimura et al. assessed seven younger patients (57–76 years), who had developed NPH after
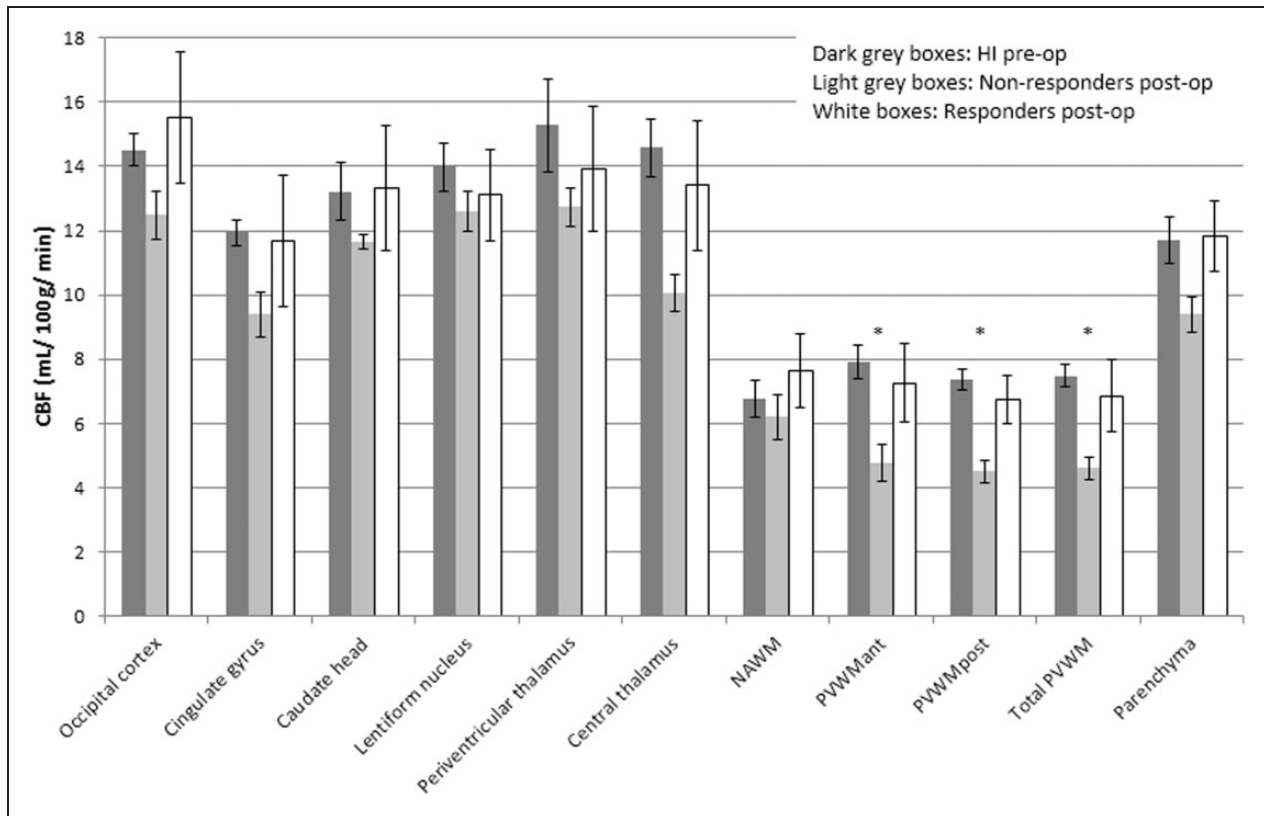
**Figure 4.** Postoperative CBF values (median, IQR) for the non-responders and the responders. The corresponding preoperative values for the healthy individuals (HI) are displayed for comparison (same data as in Figure 2). Asterisks indicate significant CBF reduction as compared to HI ($p < 0.05$).
NAWM = normal appearing white matter; PVWM = periventricular white matter; ant = anterior; post = posterior.

subarachnoid haemorrhage and had "recovered remarkably" after shunting. The study was thus biased towards very good clinical outcome and the patients' younger age and the dissimilar pathogenesis of sNPH might also have increased the chance of a high restoration ratio. Most importantly, the xenon-CT and our CTP study concordantly demonstrated the highest restoration in WM-structures. WM regions were not evaluated in a SPECT-study by Takeuchi et al.[10] that otherwise reported unique CBF restoration rates of 61% for the cortex and 86% for the thalamus-basal ganglia region.

The observed relationships in responders between perfusion of the PVWM and the cingulate gyrus and the severity of the symptoms of iNPH were in large in agreement with the findings of two previous MRP studies, which analyzed the same material.[6,11]

The present work extended the observed correlations between perfusion and clinical performance to additional anatomical regions, e.g. the parenchyma and central thalamus preoperatively and the occipital cortex pre- and postoperatively. The larger number of significant correlations in this CTP study, in spite of a

smaller sample size and a more limited spatial coverage than in the MRP evaluations, is most probably due to the use of absolute instead of relative CBF values. However, analysis of the individual changes of CBF and clinical performance after shunting resulted in no significant linear relationships in contrary to a previous MRP study.[11]

As previously discussed,[6] the WM tracts linked to gait velocity, stride length, and stride width are located close to the lateral ventricles[30] which might explain the linear relationship between PVWM CBF and the severity of gait disturbance. Also, an arterial spin labeling study measuring absolute CBF after spinal tap test showed that patients with perfusion increase in the frontal and lateral WM had a proportionally larger improvement of their gait function than patients with a perfusion decrease.[14]

The PVWM perfusion is probably also important for the functioning of the bidirectional frontal–subcortical circuits and association pathways that pass by close to the ventricular walls. These pathways are responsible for the neural transmission that supports different aspects of cognition[31] in line with our finding of a

**Table 3.** Correlations (Spearman's rho) between CBF and clinical performance in shunt responders.

| CBF (mL/ 100 g/ min) | | NP-score | Gait score | Balance score | Continence score | iNPH score |
|---|---|---|---|---|---|---|
| Occipital cortex | Pre-op | .69* | .50 | .48 | .69* | .63* |
| | Post-op | .19 | .36 | .14 | .73* | .52 |
| Cingulate gyrus | Pre-op | .68* | .61* | .48 | .65* | .67* |
| | Post-op | .16 | .57 | .17 | .67* | .61* |
| Caudate head | Pre-op | .44 | .28 | .02 | .47 | .28 |
| | Post-op | −.12 | .39 | .04 | .49 | .32 |
| Lentiform nucleus | Pre-op | .52 | .44 | .25 | .58 | .46 |
| | Post-op | .17 | .28 | .23 | .34 | .35 |
| Periventricular thalamus | Pre-op | .61 | .49 | .01 | .53 | .45 |
| | Post-op | .24 | .57 | .23 | .55 | .56 |
| Central thalamus | Pre-op | .76* | .54 | .19 | .53 | .55 |
| | Post-op | .22 | .48 | .02 | .38 | .45 |
| NAWM | Pre-op | .14 | −.06 | −.28 | .28 | .08 |
| | Post-op | −.10 | .15 | −.06 | .19 | .21 |
| PVWMant | Pre-op | .45 | .69* | .23 | .57 | .61* |
| | Post-op | .43 | .78* | .27 | .40 | .74* |
| PVWMpost | Pre-op | .45 | .69* | .23 | .57 | .61* |
| | Post-op | .09 | .47 | .17 | .59* | .52 |
| Total PVWM | Pre-op | .59* | .72* | .27 | .60* | .63* |
| | Post-op | .23 | .60* | .14 | .62* | .58* |
| Parenchyma | Pre-op | .73* | .57* | .34 | .66* | .67* |
| | Post-op | .16 | .34 | −.03 | .43 | .41 |

NP = Neuropsychology; Pre-op = preoperative; Post-op = postoperative; NAWM = Normal appearing white matter; PVWMant = anterior periventricular white matter; PVWMpost = posterior periventricular white matter; Total PVWM = PVWMant + PVWMpost. *$p < .05$.

positive correlation between PVWM CBF and neuropsychology score.

The relationship between incontinence and reduced CBF in the cingulate gyrus or the PVWM demonstrated in this study is interesting. The voluntary, inhibitory control of micturition is dependent on connections between the frontal cortex and the hypothalamus as well as between the paracentral lobule and the brainstem. Further, tonic suppression of the micturition reflex pathway seems to be exerted by the medial frontal cortex and the basal ganglia, and during voiding CBF is increased in the dorsolateral prefrontal cortex and the anterior cingulate gyrus.[32]

The anterior cingulate gyrus and the thalamus, being parts of the above mentioned frontal-subcortical circuits, mediate behavior and play a role in the regulation of overall cortical arousal[31,33] in line with the correlation between CBF in these areas and cognitive performance found in this study.

Comparing the neuropsychological performance of iNPH patients and HI, Hellström et al.[34] found that different, seemingly unrelated neuropsychological tests were associated with each other and with the level of disturbance of gait, balance and continence, indicating that widely distributed and interrelated cortical and subcortical regions participate in the generation of symptoms and signs in iNPH. The correlations between the occipital perfusion and the intensity of symptoms observed in this study might be explained by this type of co-variations.

The results of the present CTP study and of previous reports[3,5,6,11,35] may indicate that the hypoperfused periventricular WM influences multiple anatomical areas by disturbing the connections between cortical and subcortical regions. Whether this hypoperfusion is a sign of pure ischemia or secondary to metabolic downregulation remains to be investigated.

The performance of different deconvolution methods has been an object of intensive research in MRP but not in CTP. The few existing CTP studies in the matter showed that adaption of the cSVD or the block-circulant singular value decomposition using an oscillation index (oSVD)[20] to CTP data was possible and resulted in the reduction of tracer delay-induced effects.[36–38] The same studies, however, also reported remarkably variations of the absolute CBF values among the tested algorithms with the lowest estimates for cSVD.[37] Thus, the sub-physiological CBF estimates

of this work do not seem to be unique after cSVD or oSVD of CTP data, but the underlying cause is obscure. One possible explanation is the noise regularization of the deconvolution process, which in our study at 5% allowed on average only five to seven singular values to determine the form of the residue function, which probably reduced the maximum height of this curve and thereby the estimated CBF. The higher the chosen noise threshold, the more pronounced this effect will be. An optimal global noise threshold level has to our knowledge not yet been defined for CTP.

Further, the bolus injection time in CTP (12.5 s) is substantially longer than in MRP (3 s), because of the larger volume of contrast agent. As a result, the arterial and tissue attenuation-to-time curves are broad and relatively flat. The tissue residue function, convoluted over such a long time, will be very hard to estimate via deconvolution. For the context of bolus tracking MRP, Østergaard et al.[39] recommended the use of rapid bolus injections with very narrow AIF; a recommendation that is definitely not fulfilled in CTP.

In spite of the deviance of the CBF values, the absolute estimates were used for comparing statistical analyses within and between groups, because the underlying methodological bias was supposed to affect all subjects in an equivalent manner. Also, the GM-WM ratio (Table 2) was within the expected range,[40] indicating a proportional and systematic effect of the bias on grey and white matter. Relative CBF values were not used since this would confound the interpretation of the observed CBF changes.

In addition to the already mentioned factors that affect the CBF, temporal resolution, recirculation and scan duration might influence the accuracy of the hemodynamic parameters, which this study, however, controlled for. The intrinsic temporal resolution of our CTP data was not altered during post-processing and was well within the optimal range of 0.5–2 s. Recirculation effects were eliminated by fitting a model described by the gamma variate function to the attenuation-to time curves. Using a model also limited noise propagation in the calculation of the perfusion and eliminated the truncation effects of the venous output function that were noted in some of the scans.

The main weakness of this work was the small sample size, especially of the non-responder group, which reduced the power of the study and increased the variance of the results. The prime reason for the limited sample size was the ambitious study protocol that lead to the omission of subjects who had not a complete set of four successful perfusion imaging series.

Due to the limited spatial coverage of the CTP and some variation of the placement of the perfusion slab, ROIs corresponded to parts instead of to entire specific anatomical regions and showed some intra- and inter-individual variance. This supposedly increased the variance of the data. Unfortunately, at the time of the data collection, no CT-scanner with a more extended coverage was available at our center.

The choice to refrain from restricting the intake of caffeine and nicotine prior to imaging might have influenced the perfusion results. On the other hand, withdrawal of these substances and subsequent abstinence also affect the perfusion levels and is difficult to control. Therefore, the approach to let all subjects adhere to their usual intake patterns before imaging was an attempt to perform the perfusion measurements at a kind of cerebral equilibrium state.

In conclusion, CTP can be used to measure CBF changes in iNPH patients in spite of a limited spatial coverage of the technique, as demonstrated by a preoperative global and regional hypoperfusion that after shunting was reversed in responders, but remained significantly reduced in the PVWM of non-responders.

## Declaration of conflicting interests

The author(s) declared the following potential conflicts of interest with respect to the research, authorship, and/or publication of this article: Carsten Wikkelsø has received honoraria as lecturer for Johnson & Johnson Co., Raynham, MA. and Likvor AB. Remaining authors declare that they have no conflict of interest.

## Authors' contributions

All authors of this manuscript, i.e. DZ, JA, PH, MT, CW and GS, have contributed to the design of the study, the drafting of the article, and the interpretation of the results. MT, PH, and CW have been responsible for the recruitment process and the acquisition of clinical data, while DZ, GS and JA have performed the analyses of the perfusion/imaging data. All authors have approved the submission of the manuscript.

## References

1. Relkin N, Marmarou A, Klinge P, et al. Diagnosing idiopathic normal-pressure hydrocephalus. *Neurosurgery* 2005; 57: S4–S16; discussion ii–v.
2. Owler BK, Momjian S, Czosnyka Z, et al. Normal pressure hydrocephalus and cerebral blood flow: A PET study of baseline values. *J Cereb Blood Flow Metab* 2004; 24: 17–23.
3. Owler BK, Pena A, Momjian S, et al. Changes in cerebral blood flow during cerebrospinal fluid pressure manipulation in patients with normal pressure hydrocephalus: A methodological study. *J Cereb Blood Flow Metab* 2004; 24: 579–587.

4. Owler BK and Pickard JD. Normal pressure hydrocephalus and cerebral blood flow: A review. *Acta Neurol Scand* 2001; 104: 325–342.

5. Momjian S, Owler BK, Czosnyka Z, et al. Pattern of white matter regional cerebral blood flow and autoregulation in normal pressure hydrocephalus. *Brain* 2004; 127: 965–972.

6. Ziegelitz D, Starck G, Kristiansen D, et al. Cerebral perfusion measured by dynamic susceptibility contrast MRI is reduced in patients with idiopathic normal pressure hydrocephalus. *J Magn Reson Imaging* 2014; 39: 1533–1542.

7. Chang CC, Asada H, Mimura T, et al. A prospective study of cerebral blood flow and cerebrovascular reactivity to acetazolamide in 162 patients with idiopathic normal-pressure hydrocephalus. *J Neurosurg* 2009; 111: 610–617.

8. Mataro M, Poca MA, Salgado-Pineda P, et al. Postsurgical cerebral perfusion changes in idiopathic normal pressure hydrocephalus: A statistical parametric mapping study of SPECT images. *J Nucl Med* 2003; 44: 1884–1889.

9. Murakami M, Hirata Y and Kuratsu JI. Predictive assessment of shunt effectiveness in patients with idiopathic normal pressure hydrocephalus by determining regional cerebral blood flow on 3D stereotactic surface projections. *Acta Neurochir (Wien)* 2007; 149: 991–997.

10. Takeuchi T, Goto H, Izaki K, et al. Pathophysiology of cerebral circulatory disorders in idiopathic normal pressure hydrocephalus. Neurol Med Chir (Tokyo) 2007; 47: 299–306. discussion 306.

11. Ziegelitz D, Arvidsson J, Hellström P, et al. In patients with idiopathic normal pressure hydrocephalus postoperative cerebral perfusion changes measured by dynamic susceptibility contrast MRI correlate with clinical improvement. *J Comput Assist Tomogr* 2015; 39: 531–540.

12. Klinge PM, Brooks DJ, Samii A, et al. Correlates of local cerebral blood flow (CBF) in normal pressure hydrocephalus patients before and after shunting – A retrospective analysis of [(15)O]H(2)O PET-CBF studies in 65 patients. *Clin Neurol Neurosurg* 2008; 110: 369–375.

13. Corkill RG, Garnett MR, Blamire AM, et al. Multimodal MRI in normal pressure hydrocephalus identifies pre-operative haemodynamic and diffusion coefficient changes in normal appearing white matter correlating with surgical outcome. *Clin Neurol Neurosurg* 2003; 105: 193–202.

14. Virhammar J, Laurell K, Ahlgren A, et al. Idiopathic normal pressure hydrocephalus: cerebral perfusion measured with pCASL before and repeatedly after CSF removal. *J Cereb Blood Flow Metab* 2014; 34: 1771–1778.

15. Cenic A, Nabavi DG, Craen RA, et al. Dynamic CT measurement of cerebral blood flow: a validation study. *AJNR Am J Neuroradiol* 1999; 20: 63–73.

16. Kudo K, Terae S, Katoh C, et al. Quantitative cerebral blood flow measurement with dynamic perfusion CT using the vascular-pixel elimination method: comparison with H2(15)O positron emission tomography. *AJNR Am J Neuroradiol* 2003; 24: 419–426.

17. Wintermark M, Thiran JP, Maeder P, et al. Simultaneous measurement of regional cerebral blood flow by perfusion CT and stable xenon CT: A validation study. *AJNR Am J Neuroradiol* 2001; 22: 905–914.

18. Hellstrom P, Klinge P, Tans J, et al. A new scale for assessment of severity and outcome in iNPH. *Acta Neurol Scand* 2012; 126: 229–237.

19. Wahlund LO, Barkhof F, Fazekas F, et al. A new rating scale for age-related white matter changes applicable to MRI and CT. *Stroke* 2001; 32: 1318–1322.

20. Wu O, Ostergaard L, Weisskoff RM, et al. Tracer arrival timing-insensitive technique for estimating flow in MR perfusion-weighted imaging using singular value decomposition with a block-circulant deconvolution matrix. *Magn Reson Med* 2003; 50: 164–174.

21. Rempp KA, Brix G, Wenz F, et al. Quantification of regional cerebral blood flow and volume with dynamic susceptibility contrast-enhanced MR imaging. *Radiology* 1994; 193: 637–641.

22. Axel L. Cerebral blood flow determination by rapid-sequence computed tomography: Theoretical analysis. *Radiology* 1980; 137: 679–686.

23. Meier P and Zierler KL. On the theory of the indicator-dilution method for measurement of blood flow and volume. *J Appl Physiol* 1954; 6: 731–744.

24. Fedorov A, Beichel R, Kalpathy-Cramer J, et al. 3D Slicer as an image computing platform for the quantitative imaging network. *Magn Reson Imaging* 2012; 30: 1323–1341.

25. Ourselin S, Roche A, Subsol G, et al. Reconstructing a 3D structure from serial histological sections. *Image Vision Comput* 2001; 19: 25–31.

26. Ourselin S, Stefanescu R and Pennec X. Robust registration of multi-modal images: Towards real-time clinical applications. *Med Image Comput Comput-Assist Interven* 2002; 2489: 140–147.

27. Kondziella D, Sonnewald U, Tullberg M, et al. Brain metabolism in adult chronic hydrocephalus. *J Neurochem* 2008; 106: 1515–1524.

28. Kimura M, Tanaka A and Yoshinaga S. Significance of periventricular hemodynamics in normal pressure hydrocephalus. *Neurosurgery* 1992; 30: 701–704. discussion 704–705.

29. Meyer JS, Kitagawa Y, Tanahashi N, et al. Pathogenesis of normal-pressure hydrocephalus–preliminary observations. *Surg Neurol* 1985; 23: 121–133.

30. De Laat KF, Tuladhar AM, Van Norden AG, et al. Loss of white matter integrity is associated with gait disorders in cerebral small vessel disease. *Brain* 2011; 134: 73–83.

31. Tekin S and Cummings JL. Frontal-subcortical neuronal circuits and clinical neuropsychiatry: An update. *J Psychosom Res* 2002; 53: 647–654.

32. De Groat WC. A neurologic basis for the overactive bladder. *Urology* 1997; 50: 36–52. discussion 53–56.

33. Hofle N, Paus T, Reutens D, et al. Regional cerebral blood flow changes as a function of delta and spindle activity during slow wave sleep in humans. *J Neurosci* 1997; 17: 4800–4808.

34. Hellstrom P, Edsbagge M, Archer T, et al. The neuropsychology of patients with clinically diagnosed

idiopathic normal pressure hydrocephalus. *Neurosurgery* 2007; 61: 1219–1226. discussion 1227–1228.

35. Takaya M, Kazui H, Tokunaga H, et al. Global cerebral hypoperfusion in preclinical stage of idiopathic normal pressure hydrocephalus. *J Neurol Sci* 2010; 298: 35–41.

36. Kudo K, Sasaki M, Ogasawara K, et al. Difference in tracer delay-induced effect among deconvolution algorithms in CT perfusion analysis: Quantitative evaluation with digital phantoms. *Radiology* 2009; 251: 241–249.

37. Sasaki M, Kudo K, Ogasawara K, et al. Tracer delay-insensitive algorithm can improve reliability of CT perfusion imaging for cerebrovascular steno-occlusive disease: comparison with quantitative single-photon emission CT. *AJNR Am J Neuroradiol* 2009; 30: 188–1893.

38. Wittsack HJ, Wohlschlager AM, Ritzl EK, et al. CT-perfusion imaging of the human brain: advanced deconvolution analysis using circulant singular value decomposition. *Comput Med Imaging Graph* 2008; 32: 67–77.

39. Ostergaard L, Weisskoff RM, Chesler DA, et al. High resolution measurement of cerebral blood flow using intravascular tracer bolus passages. Part I: Mathematical approach and statistical analysis. *Magn Reson Med* 1996; 36: 715–725.

40. Wirestam R, Andersson L, Ostergaard L, et al. Assessment of regional cerebral blood flow by dynamic susceptibility contrast MRI using different deconvolution techniques. *Magn Reson Med* 2000; 43: 691–700.